



School of Computing, Computational PDEs Unit
<http://www.comp.leeds.ac.uk/scicomp/>

The Greatest Hits of EHL

Elyas Nurgat, Chris Goodyer, Dan Hart

Hongqiang Lu, Elham Afandizadeh Zargari

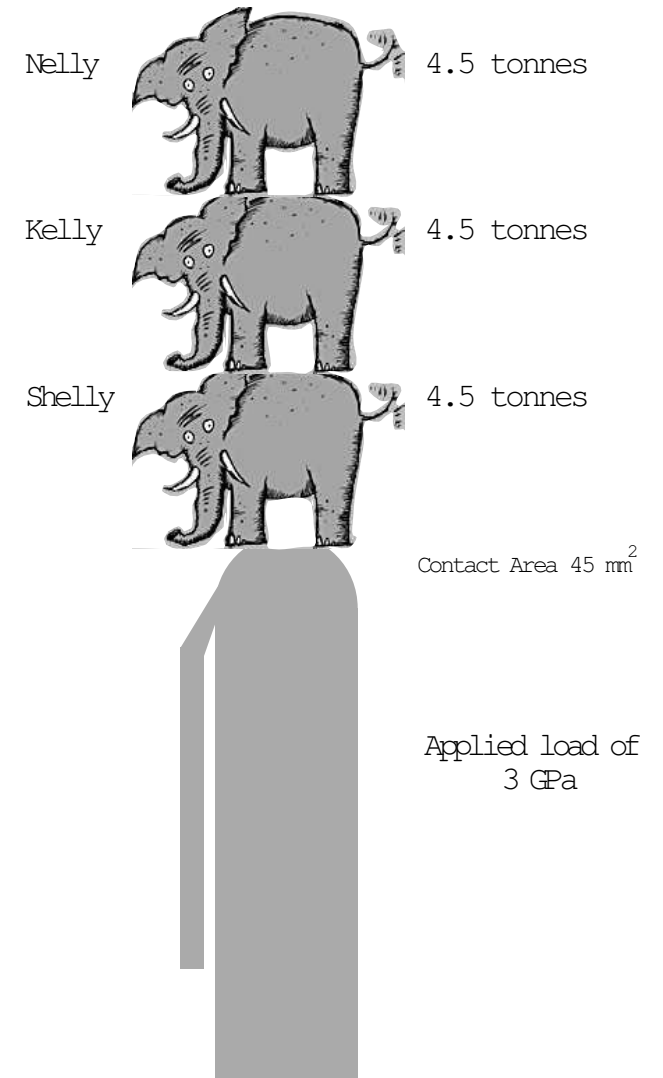
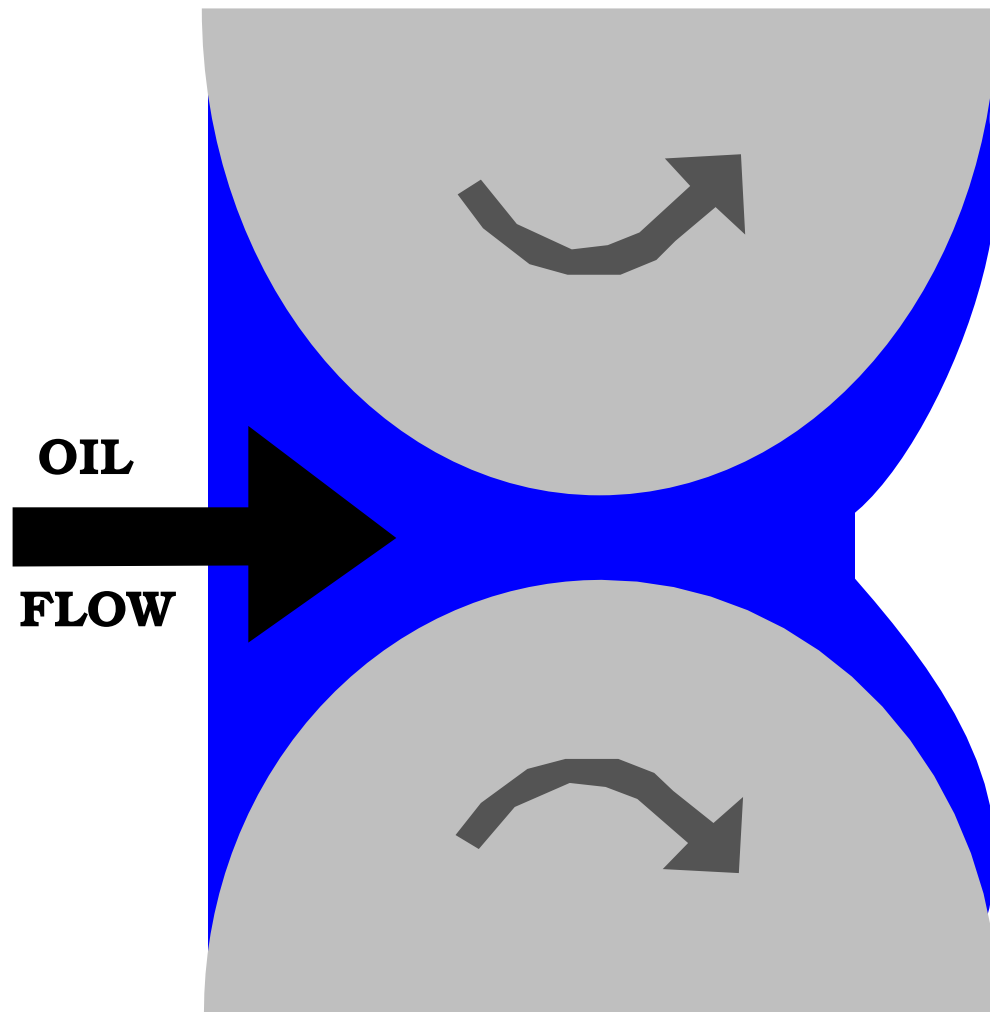
Roger Fairlie, Mark Walkley

Martin Berzins, Peter Jimack

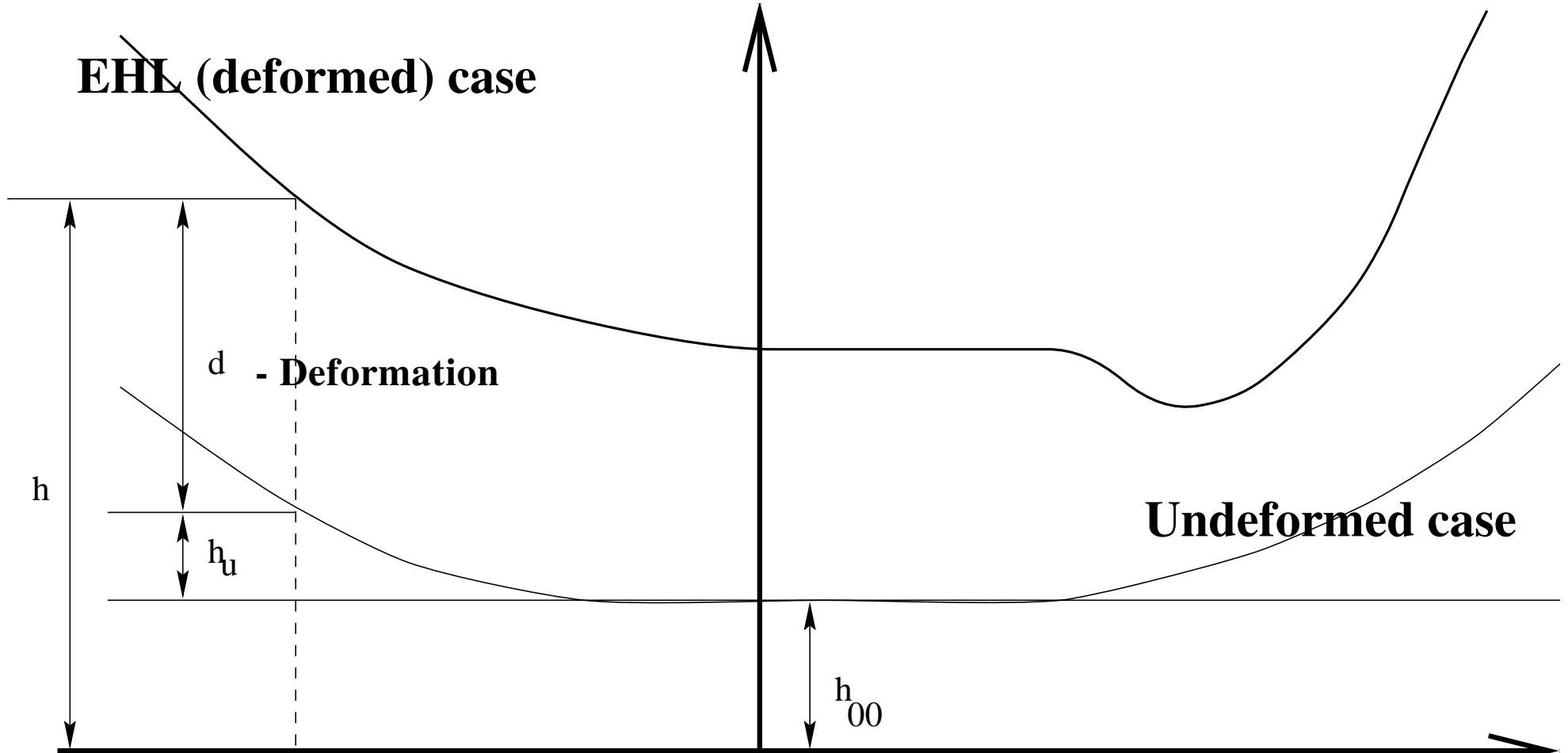
Laurence Scales (Shell Global Solutions)

Lubrication

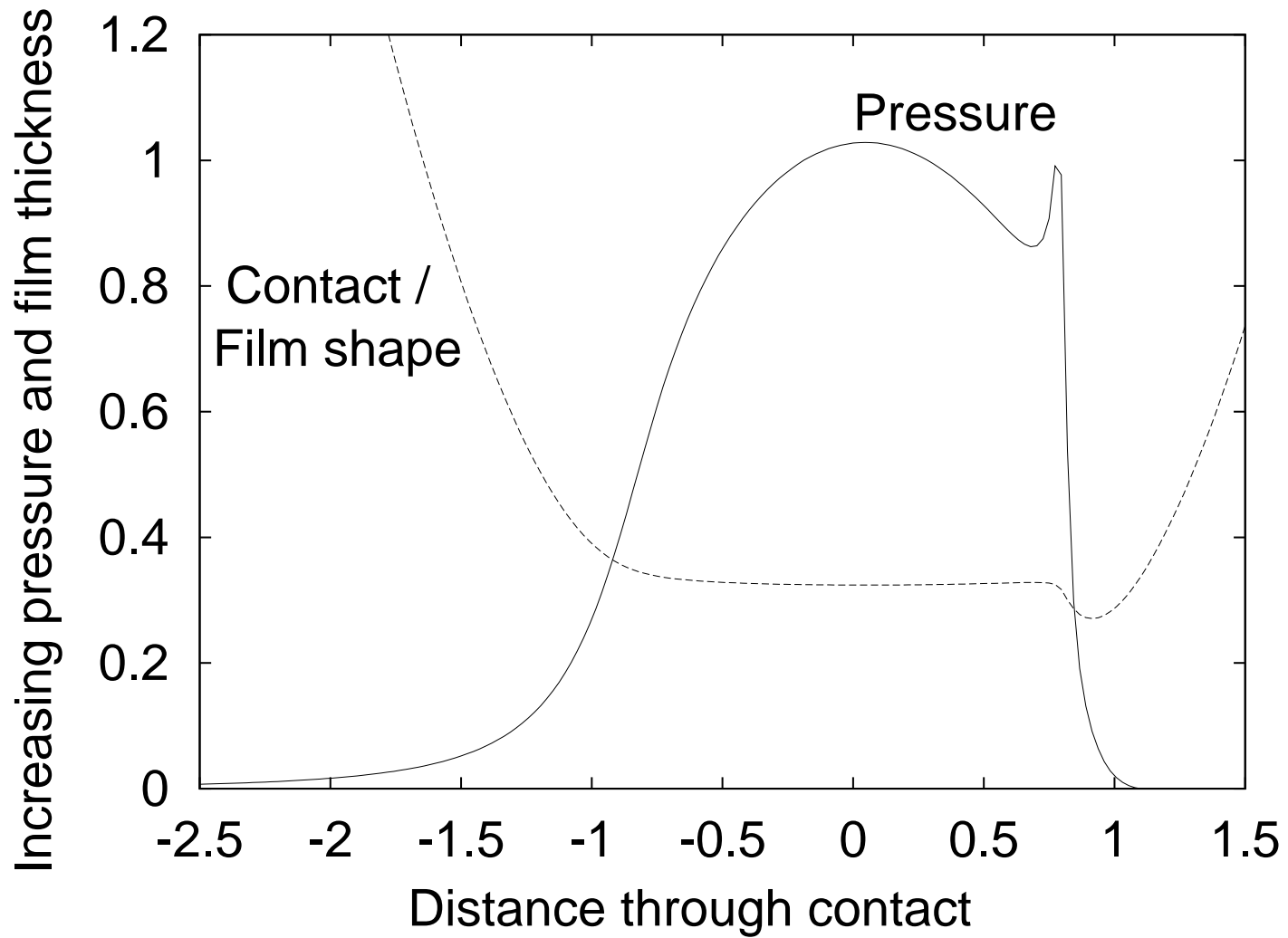
A hydrodynamic contact



(Elasto)hydrodynamic Lubrication Contacts



Geometry and Pressure plots across an EHL contact



Governing Equations I :

The Reynolds Equation

$$\frac{\partial}{\partial x} \left(\frac{\rho h^3}{\eta} \frac{\partial p}{\partial x} \right) + \frac{\partial}{\partial y} \left(\frac{\rho h^3}{\eta} \frac{\partial p}{\partial y} \right) = 6 \left\{ u_s \frac{\partial (\rho h)}{\partial x} + v_s \frac{\partial (\rho h)}{\partial y} + \rho h \frac{\partial u_s}{\partial x} + \rho h \frac{\partial v_s}{\partial y} + 2 \frac{\partial (\rho h)}{\partial t} \right\}$$

where,

p is the pressure, h is the film thickness, η is the viscosity,

ρ is the density, t is the time, x, y Cartesian coordinates

and u_s, v_s are the surface velocities in the x and y directions respectively.

Governing Equations II :

The Film Thickness Equation

1D line contact:

$$h(x, y) = h_{00} + \frac{x^2}{2R_x} + \frac{4}{\pi E'} \int_{-\infty}^{\infty} \ln \left| \frac{x - x'}{x_0} \right| p(x') dx'$$

2D circular point contact:

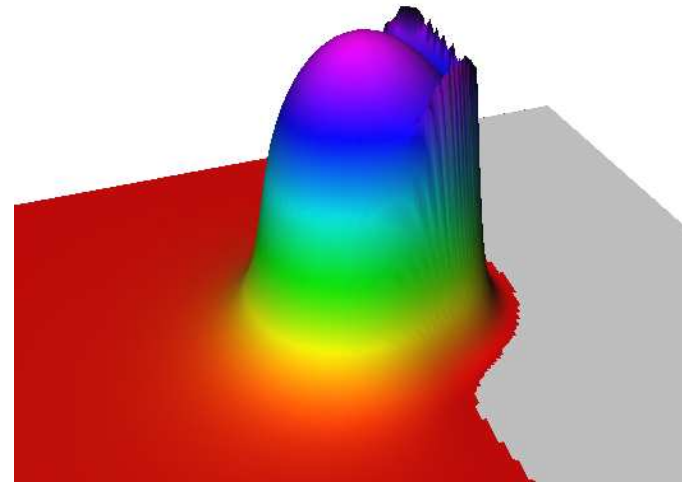
$$h(x, y) = h_{00} + \frac{x^2}{2R_x} + \frac{y^2}{2R_y} + \frac{2}{\pi E'} \int_{-\infty}^{\infty} \int_{-\infty}^{\infty} \frac{p(x', y') dx' dy'}{\sqrt{(x - x')^2 + (y - y')^2}},$$

Film thickness, h , at a point depends upon all the pressures!

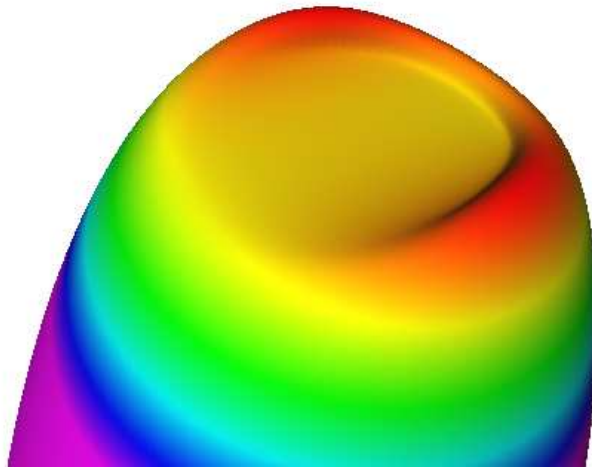
Conservation law - applied load carried entirely by lubricant film:

$$\int_{-\infty}^{\infty} \int_{-\infty}^{\infty} p(x, y) dx dy = F$$

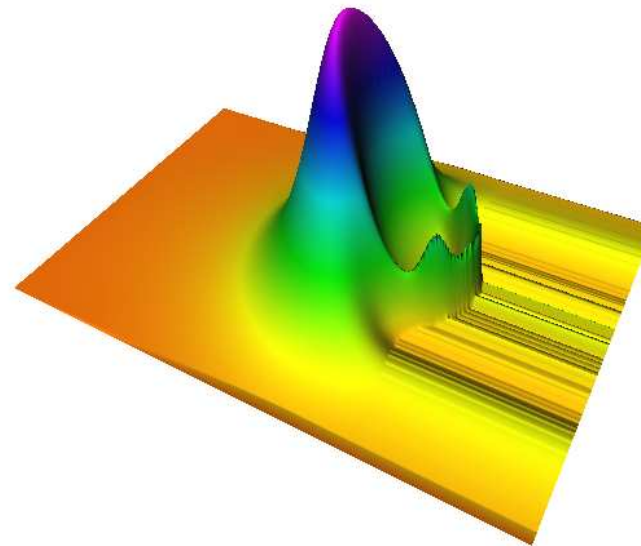
Typical solutions



Pressure



Film thickness



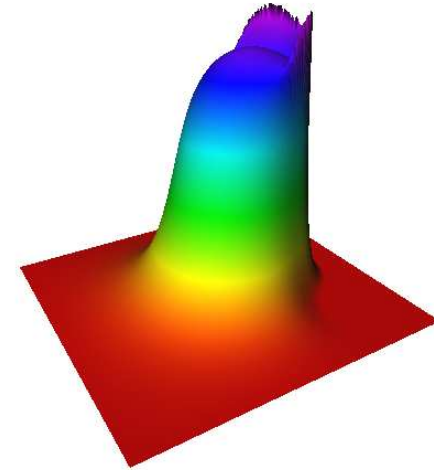
Temperature

Governing Equations III : Lubricant model (isothermal)

Density model: (Dowson and Higginson)

$$\rho(p) = \rho_0 \left(1 + \frac{5.8 \times 10^{-10} p}{1 + 1.7 \times 10^{-9} p} \right)$$

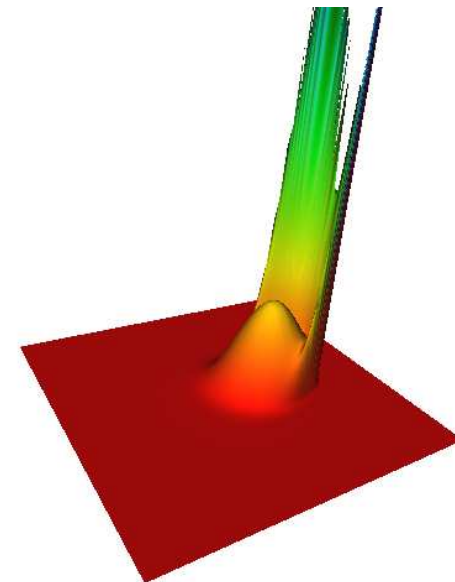
[Pictured non-dimensional range 1 → 1.16]



Viscosity Model: (from Roelands equation)

$$\eta(p) = \eta_0 \exp \left\{ \frac{\alpha p_0}{z} \left[-1 + \left(1 + \frac{p}{p_0} \right)^z \right] \right\}$$

[Pictured non-dimensional range 1 → 13300]



- More realistic rheological (non-Newtonian models) may be used instead

Governing Equations IV :

The Energy Equation

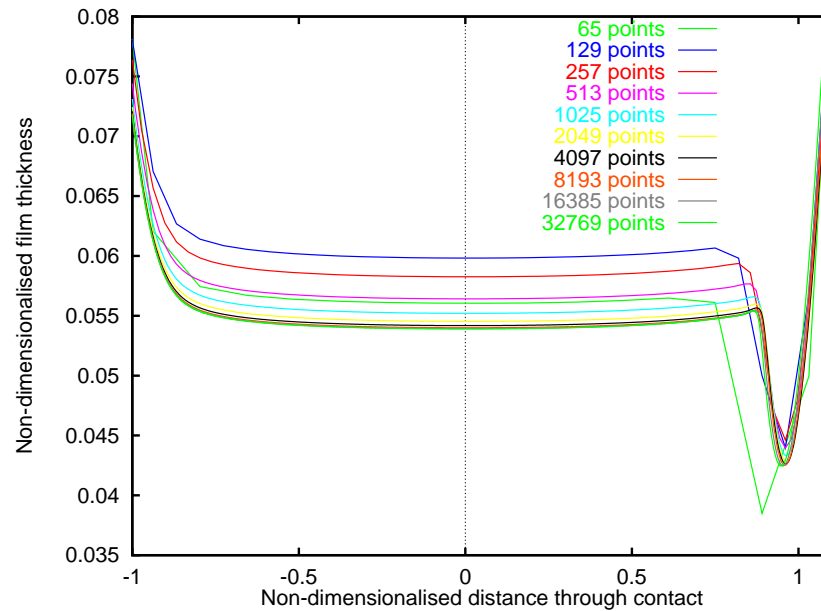
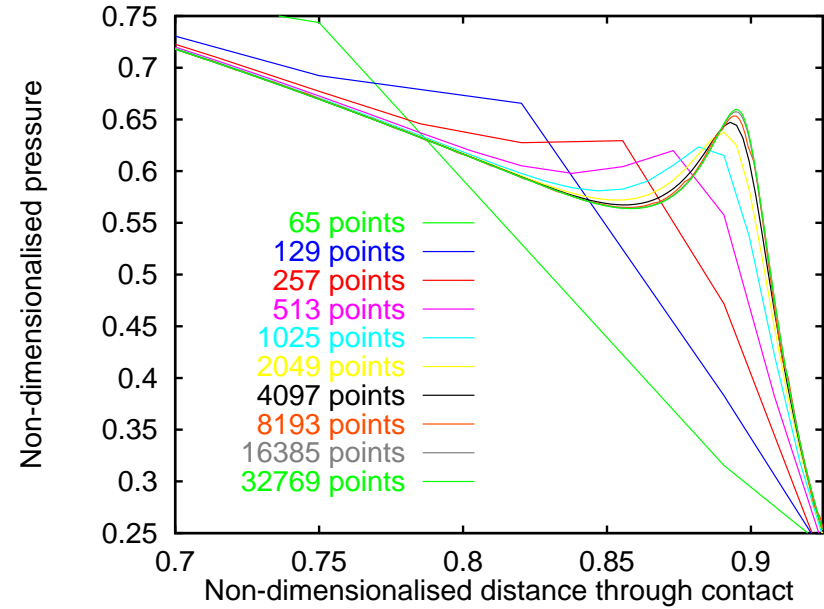
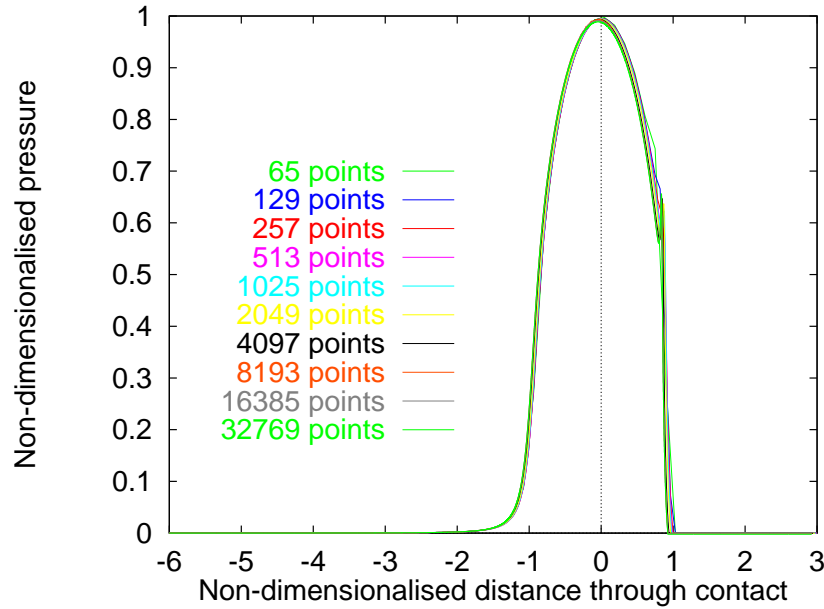
For thermal cases the Energy Equation also applies:

$$\rho \left\{ \frac{1}{2} \frac{\partial \theta}{\partial T} + U_m \frac{\partial \theta}{\partial X} + V_m \frac{\partial \theta}{\partial Y} + \frac{\theta - \theta_b}{H} \left[(U_m - U_b) \frac{\partial H}{\partial X} + V_m \frac{\partial H}{\partial Y} \right] \right\} =$$
$$\frac{3k}{2B^2H^2} (\theta_a + \theta_b - 2\theta) + \beta_e \theta \left(\frac{1}{2} \frac{\partial P}{\partial T} + U_m \frac{\partial P}{\partial X} + V_m \frac{\partial P}{\partial Y} \right) -$$
$$2B\mu \left[\left(U_m - \frac{U_e}{2} \right) \frac{\partial P}{\partial X} - V_m \frac{\partial P}{\partial Y} \right] + \frac{B\mu\kappa}{3} \eta \Gamma_m^2$$

with the two surface temperatures given in the form

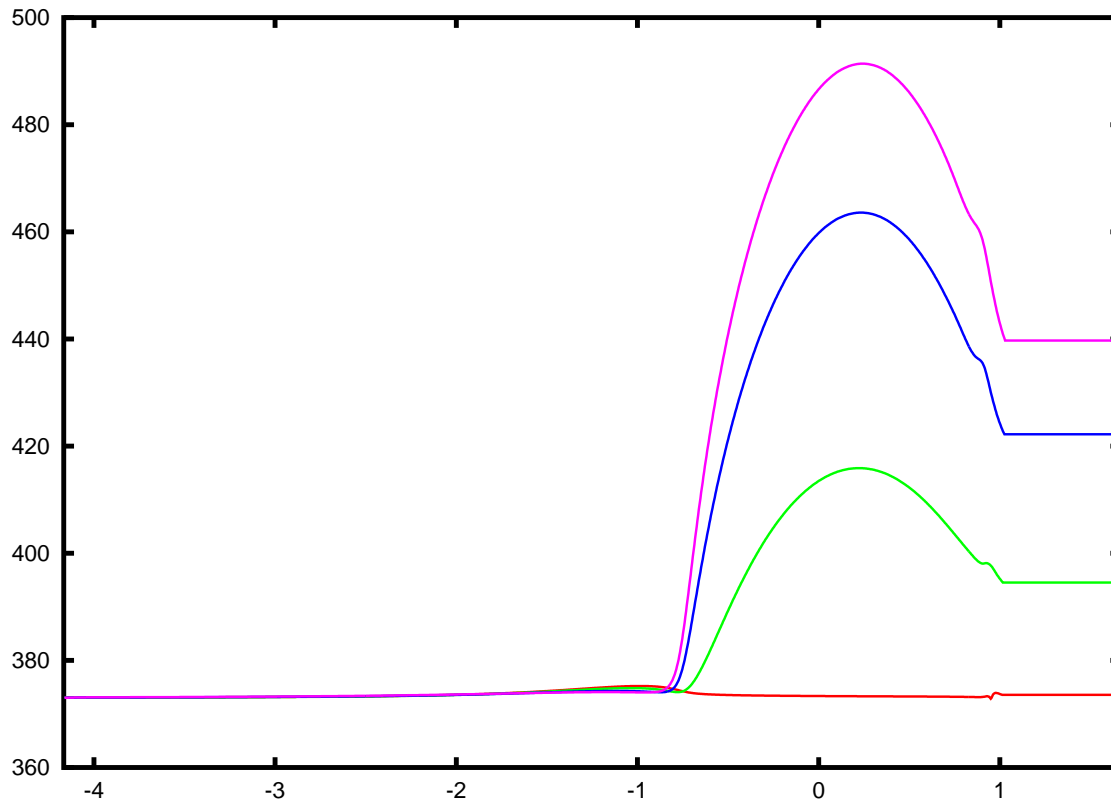
$$\theta_a(X) = 1 + 2\kappa\chi_a \int_{-\infty}^X \frac{(3\theta - 2\theta_a - \theta_b)d\zeta}{H(X)\sqrt{X - \zeta}}$$

Line Contact - Pressure Spike Resolution



Line Contact - Thermal Slide to Roll Ratios

Temperature across domain



Slide to roll ratio given by

$$\mathcal{S} = \frac{2(u_2 - u_1)}{u_1 + u_2}$$

where u_1 and u_2 are the rolling velocities of the two surfaces.

Shown is the same example as the previous slide with pure rolling ($\mathcal{S}=0$) in red, with increasing shear ($\mathcal{S} = 0.34, 1, 1.4$).

Standard EHL Solution Methods

Finite differences on a regular mesh using multigrid

- Solve (non-linear) Reynolds equation for new Pressure
 - Contact Region solution schemes include:
 - * Distributive scheme [Lubrecht & Venner]
 - * Jacobi Line [Nurgat & Berzins]
 - Non-contact region - G-S Line scheme
 - Cavitation Region - Reynolds Equation not valid
- Update H using new P
 - Computationally expensive but **Multilevel Multi-integration** substantially reduces work
- Update Density and Viscosity
- Evaluate Energy Equation by pointwise Jacobi along each line
- H_{00} once per multigrid cycle through relaxation of force balance equation

Point Contact - Discretisation I

The Reynolds Equation:

$$\begin{aligned} \frac{1}{\Delta T} (\bar{\rho}_{i,j} H_{i,j} - \bar{\rho}_{i,j}^{t-1} H_{i,j}^{t-1}) &= \frac{1}{\Delta X^2} \left[\varepsilon_{i+\frac{1}{2},j} (P_{i+1,j} - P_{i,j}) - \varepsilon_{i-\frac{1}{2},j} (P_{i,j} - P_{i-1,j}) \right] \\ &+ \frac{1}{\Delta Y^2} \left[\varepsilon_{i,j+\frac{1}{2}} (P_{i,j+1} - P_{i,j}) - \varepsilon_{i,j-\frac{1}{2}} (P_{i,j} - P_{i,j-1}) \right] \\ &- \frac{1}{\Delta X} (\bar{\rho}_{i,j} H_{i,j} - \bar{\rho}_{i-1,j} H_{i-1,j}) \end{aligned}$$

where

$$\varepsilon_{i,j} = \frac{\bar{\rho}_{i,j} H_{i,j}^3}{\bar{\eta}_{i,j} \lambda}$$

The Force Balance Equation:

$$\Delta X \Delta Y \sum_{i=1}^{N_X} \sum_{j=1}^{N_Y} P_{i,j} = \frac{2\pi}{3}$$

Point Contact - Discretisation II

The Film Thickness Equation:

$$H_{i,j} = H_{00} + \frac{X_i^2}{2} + \frac{Y_j^2}{2} - \frac{2}{\pi^2} \sum_{k=1}^{N_X} \sum_{l=1}^{N_Y} K_{i,j,k,l} P_{k,l}$$

$$\text{where } K_{i,j,k,l} = \frac{2}{\pi^2} \left\{ \begin{aligned} &|X_p| \sinh^{-1} \left(\frac{Y_p}{X_p} \right) + |Y_p| \sinh^{-1} \left(\frac{X_p}{Y_p} \right) \\ &- |X_m| \sinh^{-1} \left(\frac{Y_p}{X_m} \right) - |Y_p| \sinh^{-1} \left(\frac{X_m}{Y_p} \right) \\ &- |X_p| \sinh^{-1} \left(\frac{Y_m}{X_p} \right) - |Y_m| \sinh^{-1} \left(\frac{X_p}{Y_m} \right) \\ &+ |X_m| \sinh^{-1} \left(\frac{Y_m}{X_m} \right) + |Y_m| \sinh^{-1} \left(\frac{X_m}{Y_m} \right) \end{aligned} \right\}$$

Point Contact - Discretisation III

The Energy Equation:

$$\rho_i \left\{ \frac{\theta_{i,j} - \theta_{i,j}^{t_{n-1}}}{2\Delta T} + U_m \frac{\theta_{i,j} - \theta_{i-1,j}}{\Delta X} + \frac{\theta_{i,j} - \theta_b}{H_{i,j}} \left[(U_m - U_b) \frac{H_{i,j} - H_{i-1,j}}{\Delta X} + V_m \frac{H_{i,j} - H_{i,j-1}}{\Delta Y} \right] \right\}$$

$$= \frac{3k}{2B^2 H_{i,j}^2} (\theta_a + \theta_b - 2\theta_{i,j}) + \beta_e \theta_{i,j} \left[\frac{P_{i,j} - P_{i-1,j}^{t_{n-1}}}{2\Delta T} + U_m \frac{P_{i,j} - P_{i-1,j}}{\Delta X} + V_m \frac{P_{i,j} - P_{i,j-1}}{\Delta Y} \right] -$$

$$2B\mu \left[\left(U_m - \frac{U_e}{2} \right) \frac{P_{i,j} - P_{i-1,j}}{\Delta X} - V_m \frac{P_{i,j} - P_{i,j-1}}{\Delta Y} \right] + \frac{B\mu\kappa}{3} \eta_{i,j} \Gamma_m^2$$

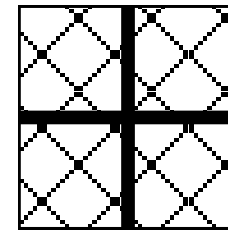
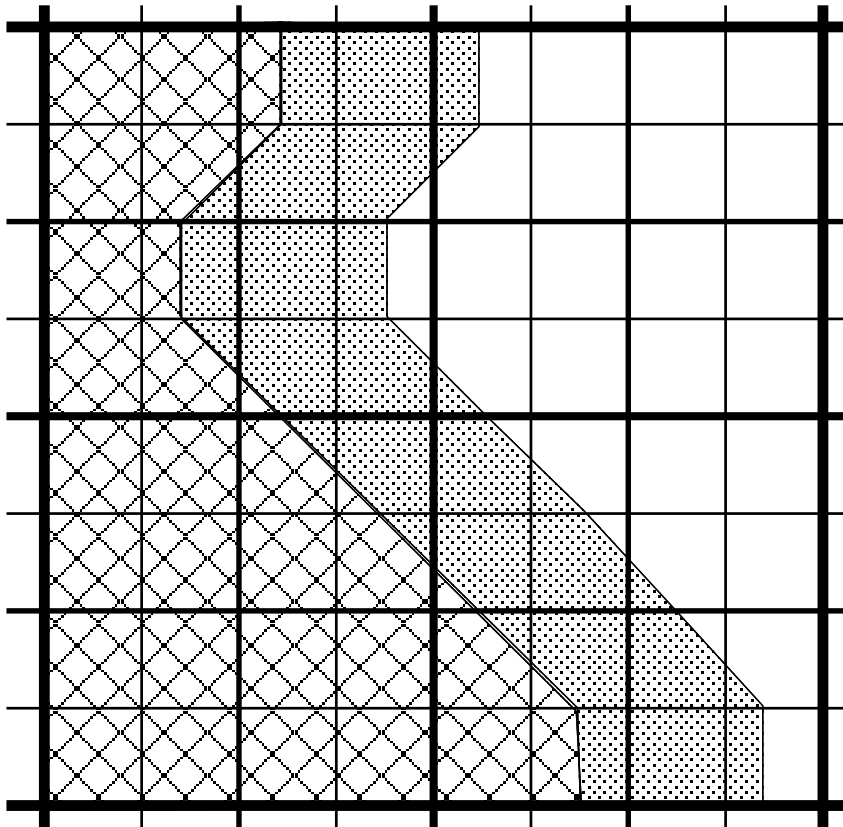
where

$$U_m = -\frac{H_{i,j}^2}{2\kappa\eta_{i,j}} \frac{P_{i,j} - P_{i,j-1}}{\Delta X} + \frac{U_e}{2} \quad \text{and} \quad V_m = \frac{H_{i,j}^2}{2\kappa\eta_{i,j}} \frac{P_{i,j} - P_{i,j-1}}{\Delta Y}$$

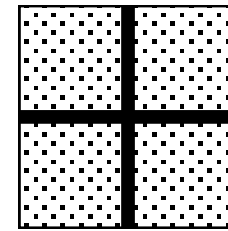
The Surface Temperature Equation:

$$\theta_{a;i,j} = 1 + 4\kappa\chi_a \sum_{k=1}^i \left[\frac{\theta_{A;k-1,j} + \theta_{A;k,j}}{H_{k-1,j} + H_{k,j}} \left(\sqrt{X_k - X_{k-1}} - \sqrt{X_i - X_k} \right) \right]$$

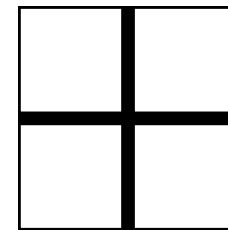
Grid Adaptation - Free boundary treatment



Pressure positive
point



Cavitation point
included in
adaptive solve

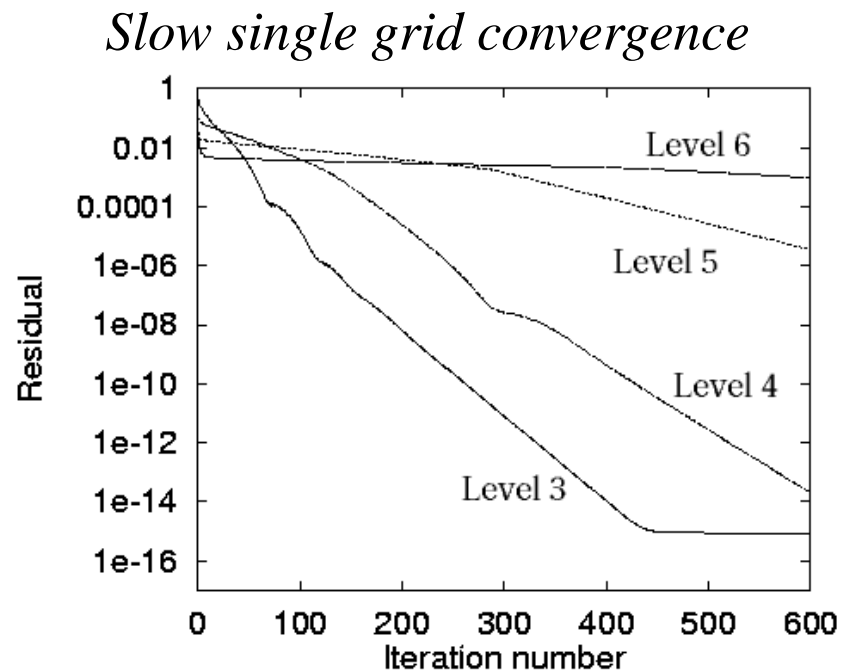


Cavitation point
excluded from
adaptive solve

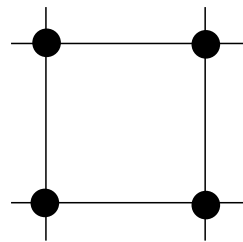
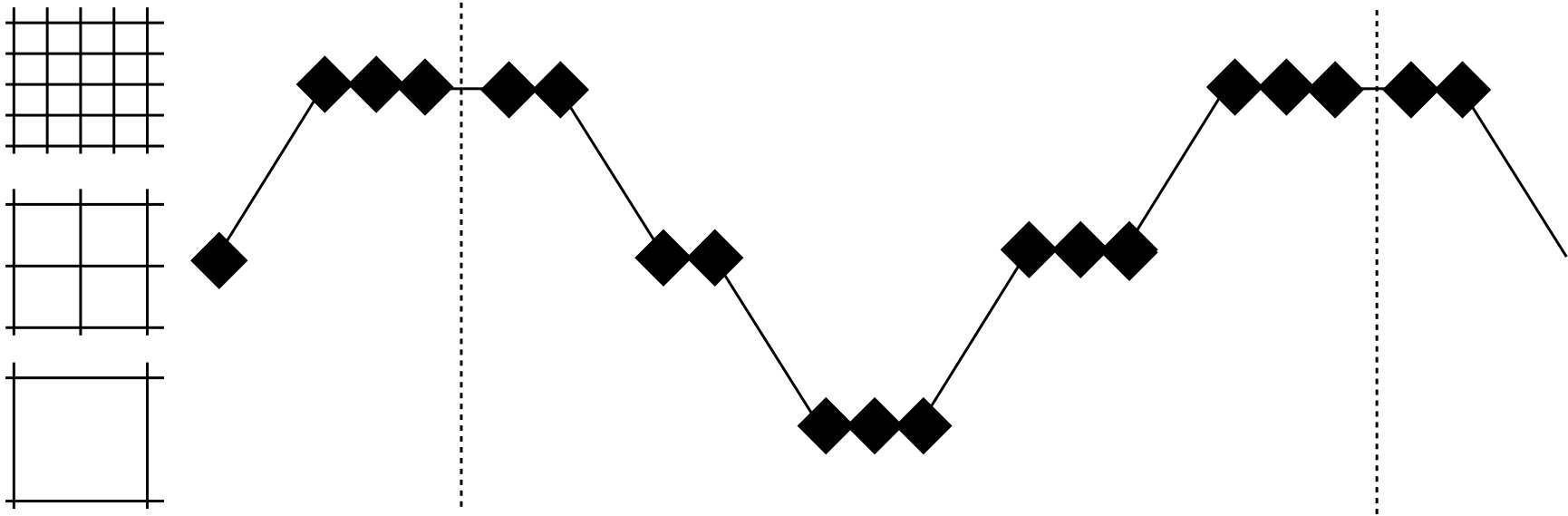
At least one point inside the cavitation region (zero pressure) included in each pressure solve

Multigrid

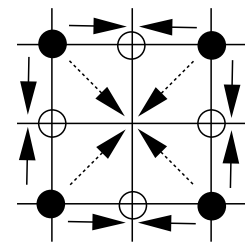
- Standard iterative methods good at removing high frequency errors relative to grid
- Bad at removing low frequency errors relative to grid
- Use of multiple levels of grid refinement accelerate convergence on fine grids
- On fine meshes more of the errors are low frequency relative to grid



Multigrid Cycles

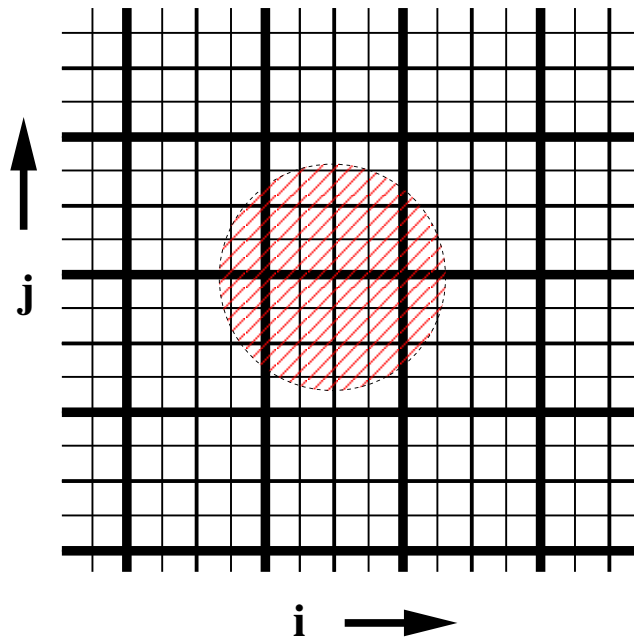


Prolongation \rightarrow
 \leftarrow Coarsening



Adaptive multigrid may be used...

Multilevel Multi-Integration



- Aim is to reduce work by summing over as few elements as possible
- Sum over fine grid points near singularity
- Add sum from all coarse grid points
- Correct in region of influence

$$H_{i,j} = H_{00} + \frac{X_i^2}{2} + \frac{Y_j^2}{2} - \frac{2}{\pi^2} \sum_{k=1}^{N_X} \sum_{l=1}^{N_Y} K_{i,j,k,l} P_{k,l}$$

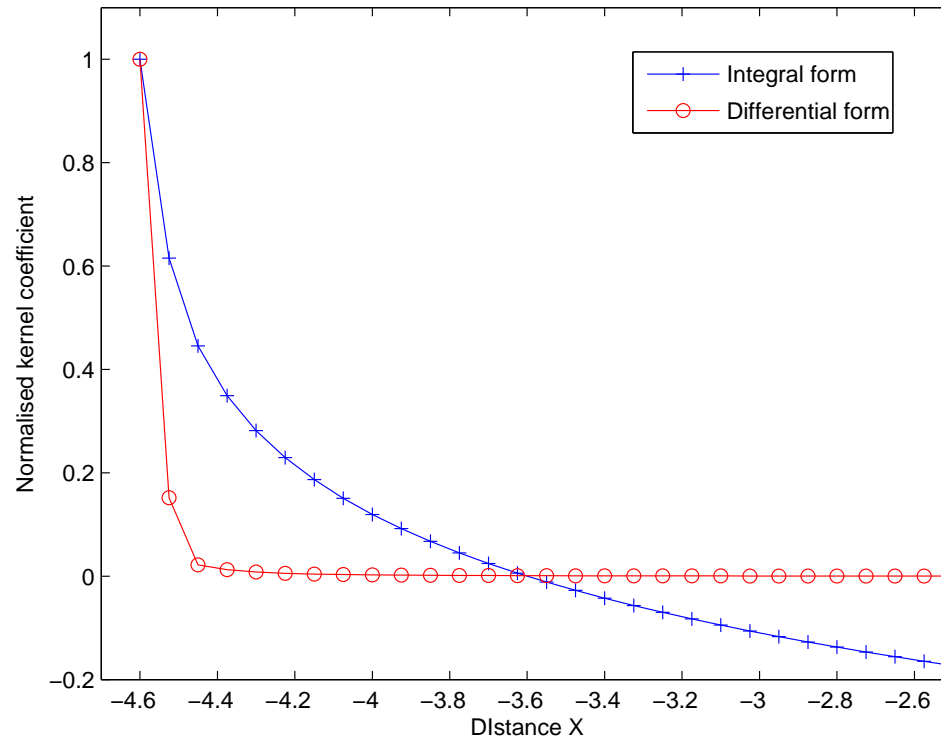
This is similar to the fast multipole method

Differential Deflection Method

Reformulates the integral Film Thickness equation as a differential equation

$$\frac{\partial^2 H}{\partial X^2} = 1 - \sum_j (f_j p_j)$$

The new kernel f_j is more “local” and hence more efficient computationally



NB: DDM kernel rapidly approaches 0; the basic kernel is non-zero everywhere

Point Contact - MLMI Speed-ups

MLMI computational times (s) for a single film thickness calculation

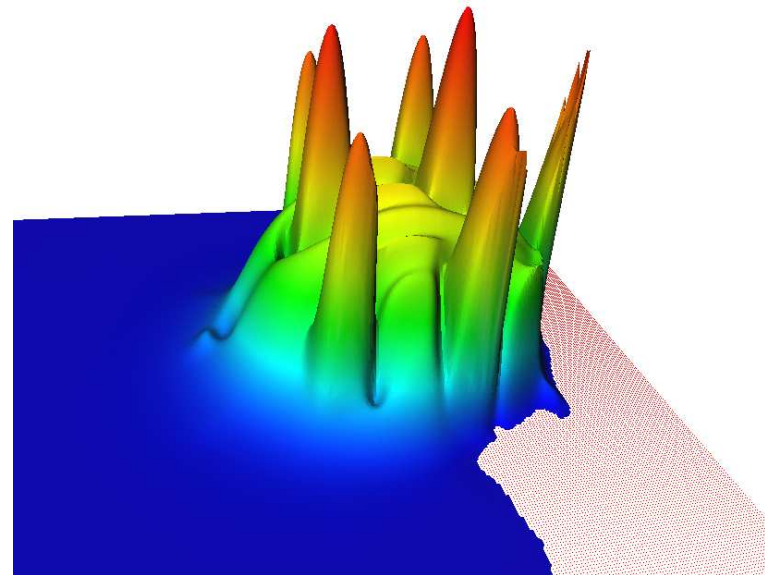
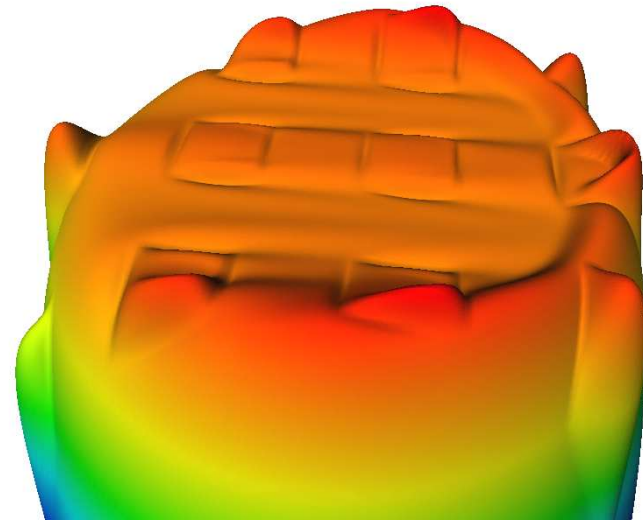
		Coarsest grid used in multi-integration				
		Level 3	Level 4	Level 5	Level 6	Level 7
Level	5	0.14	0.22	2.29	-	-
of	6	0.35	0.50	2.30	28.5	-
solution	7	1.14	1.26	3.21	28.2	397

Root mean square error of a typical calculation

		Level 3	Level 4	Level 5	Level 6
Level	5	3.2×10^{-5}	1.2×10^{-5}	-	-
of	6	3.5×10^{-5}	1.8×10^{-5}	7.2×10^{-6}	-
solution	7	3.7×10^{-5}	2.1×10^{-5}	1.0×10^{-5}	3.8×10^{-6}

Surface Roughness

- Real surfaces are not smooth
- Surface geometry can now be measured
- Detail requires very fine meshes - hence fast solvers
- Important in applications where gap is very narrow
- All roughness problems *transient*

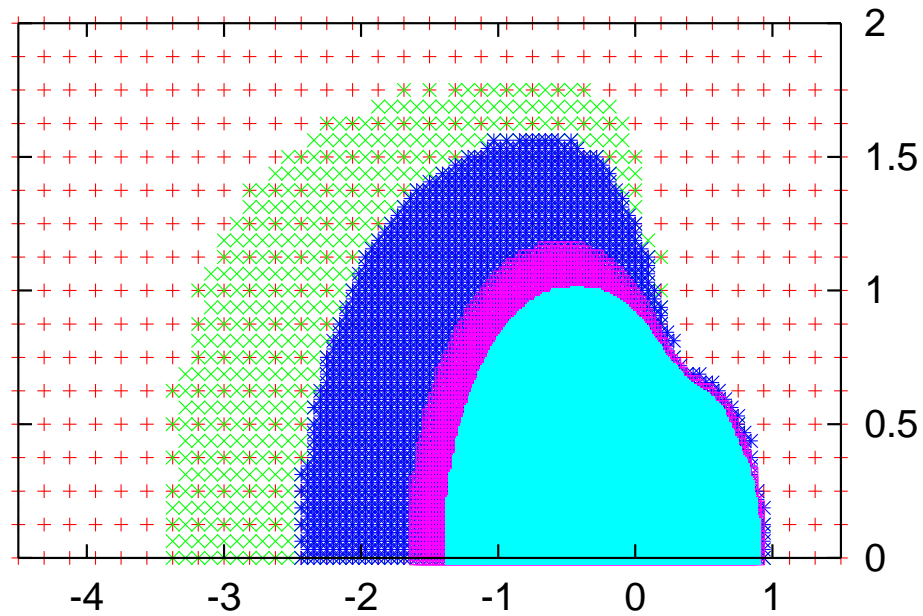


Grid Adaptation

- EHL calculations are very expensive on fine meshes
- Interesting behaviour restricted to the contact area
- Inlet region very important for good solutions
- Adaptive meshing allows solutions of similar accuracy, but cheaper
- Refine based on either:
 - pre-defined geometry
 - monitor function, e.g. pressure
 - error test
 - adjoint calculation...
- Work concentrated where needed

Deformation calculation not yet done on an adapted mesh

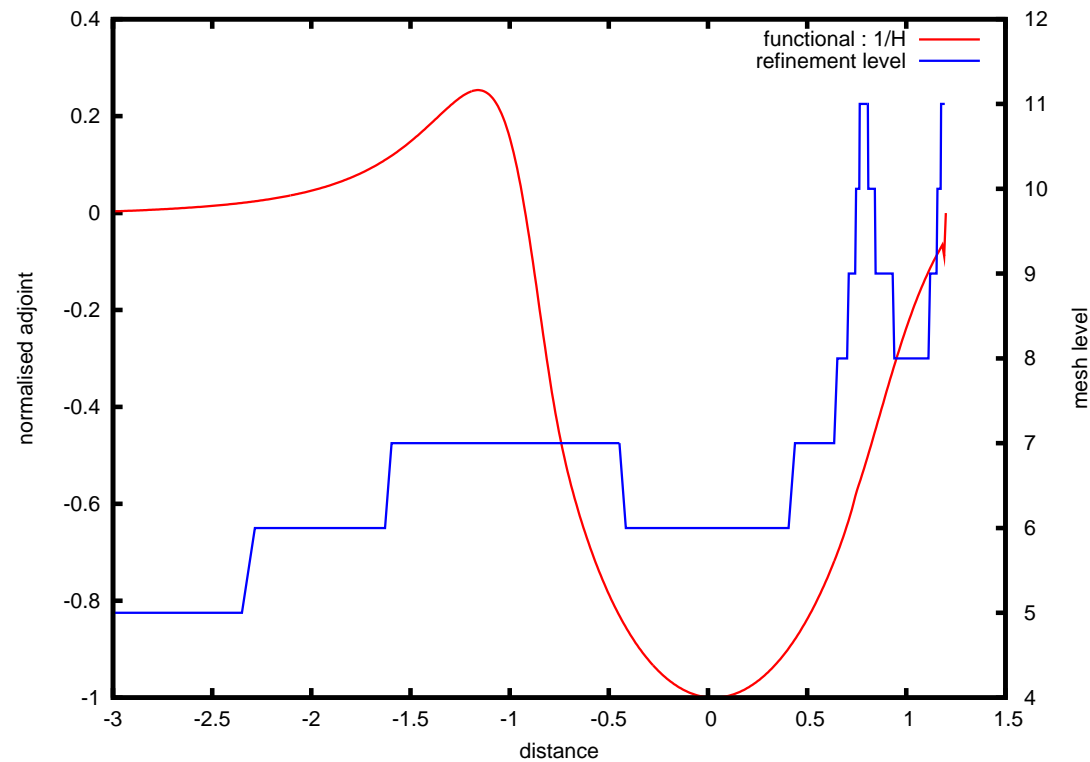
2-d Grid Adaptation - Results



Grid dimension	Adaptation style	Speed up
129×129	Geometry	37.7%
257×257	Monitor function	49.9%
513×513	Error test	48.8%

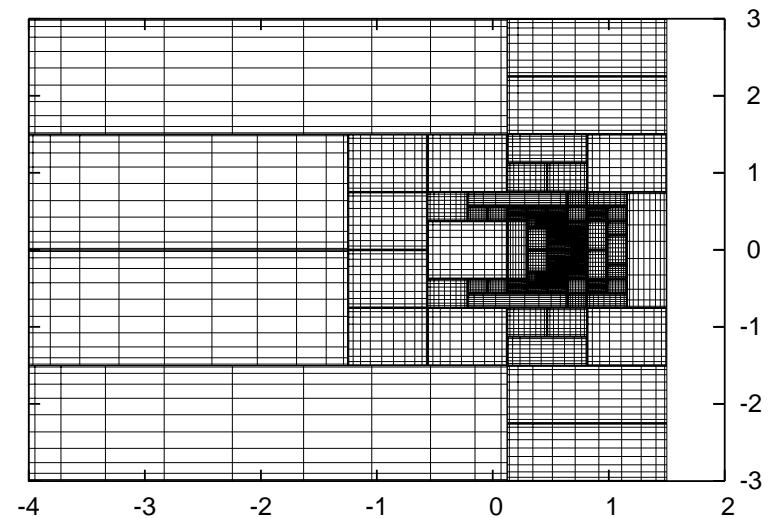
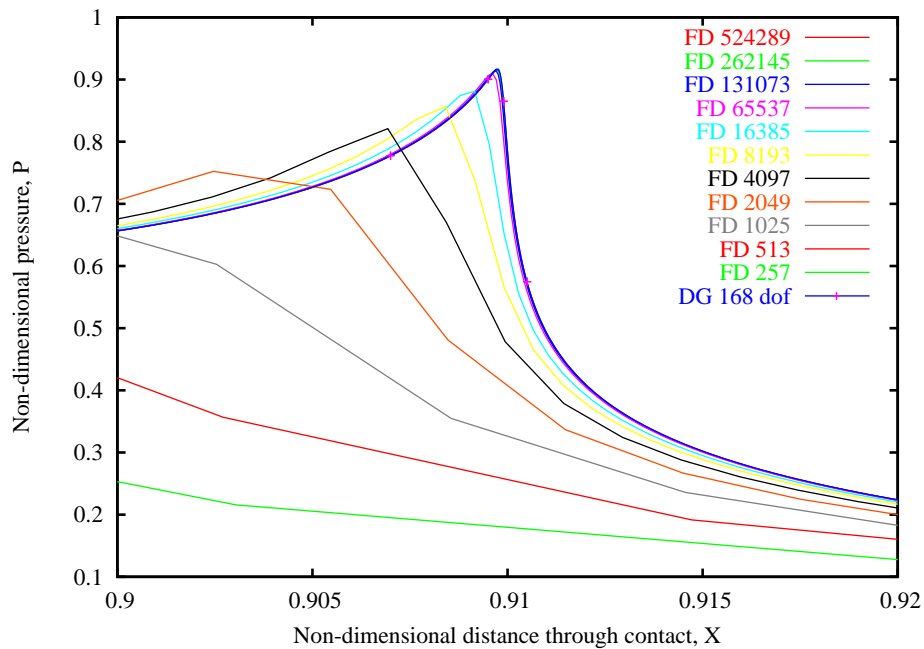
1-d Adaptation using Adjoint Calculations

- Friction is a **quantity of interest**
- Adjoint solve is lightweight and gives sensitivity to the QoI
- Can undertake refinement to get friction accurately



Discontinuous Galerkin Finite Elements

- Uses finite elements – normally not very stable for EHL
- High order polynomials are used - 9th order or more
- High accuracy from small number of unknowns
- Adaptivity may be in both space and order



Transient EHL Problems

- EHL is an inherently transient field
- Novel use of a standard ODE solver coupled with standard convergence test linked to MG solver
- Continue iterations to reduce errors using Shampine convergence test:

$$\frac{\sigma}{1 - \sigma} \left\| \underline{H}^{(m+1)}(t_n) - \underline{H}^{(m)}(t_n) \right\| < 0.33tol$$

where tol is an error tolerance for the iteration, $\| \cdot \|$ a suitable norm, m the multigrid iteration number, and σ is an estimate of the rate of convergence

- Use of standard ODE techniques to predict next timestep solutions

Differential Algebraic Formulation

In discretised form, for solution vectors \underline{P} , \underline{H} and $\underline{\rho}$, the system can be written:

$$\text{Reynolds Equation: } \underline{F}(\underline{P}, \underline{\rho H}, [\underline{\rho \dot{H}}]) = 0$$

$$\text{Film thickness: } \underline{H} = \underline{h}_0 + K\underline{P}$$

K is a large dense block Toeplitz (non-singular?) matrix

There is no explicit transient derivative of pressure, hence this is not an ODE but a DAE system

Assuming non-singularity this has DAE index 1

Variable Time Stepping using Local Error Control

- Define the local errors in \underline{H} and \underline{P} by \underline{leH} and \underline{leP}

- Standard error equations in DAE form [Petzold]

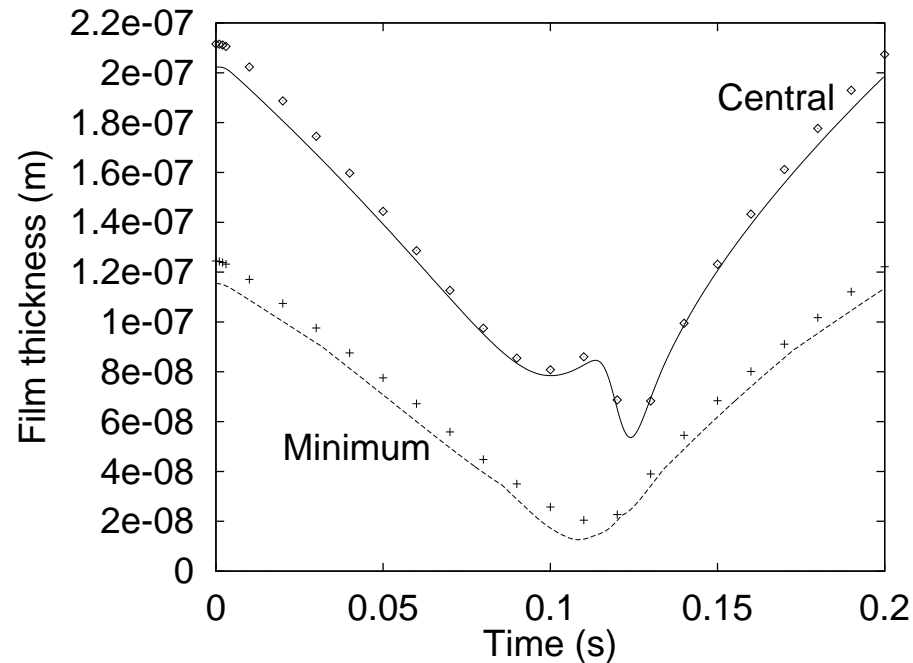
$$\begin{bmatrix} -1 - \Delta T \frac{\partial \underline{F}_1}{\partial \underline{\rho H}} & -\Delta T \frac{\partial \underline{F}_1}{\partial \underline{P}} \\ -\Delta T & \Delta T K \end{bmatrix} \begin{bmatrix} \underline{leH} \\ \underline{leP} \end{bmatrix} = \begin{bmatrix} -1 & 0 \\ 0 & 0 \end{bmatrix} \frac{1}{2} \begin{bmatrix} \underline{H}_n - \underline{H}_n^{pred} \\ \underline{P}_n - \underline{P}_n^{pred} \end{bmatrix}$$

- This gives $\underline{leH} = K \underline{leP}$ and the standard estimate for the local error:

$$-\Delta T \left(\frac{\underline{leH}}{\Delta T} + \frac{\partial \underline{F}_1}{\partial \underline{\rho H}} \underline{leH} + \frac{\partial \underline{F}_1}{\partial \underline{P}} \underline{leP} \right) = -\frac{(\underline{H}_n - \underline{H}_n^{pred})}{2}$$

Transient EHL Problem - Reversal

- Models mechanical situations where engine parts move, eg cams, gears
- Entrainment velocity slows down • Goes through 0ms^{-1} at 0.1s
- Speeds up in opposite direction

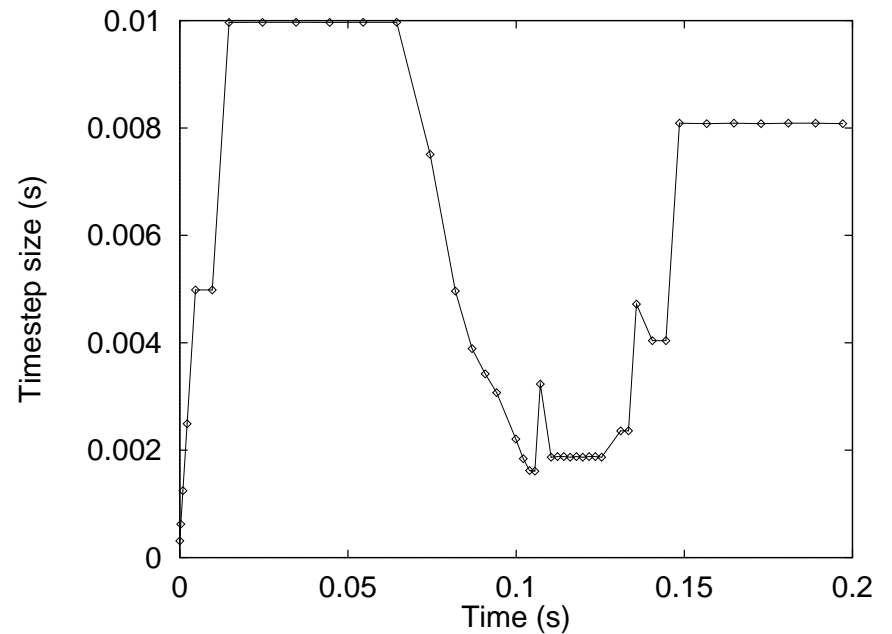
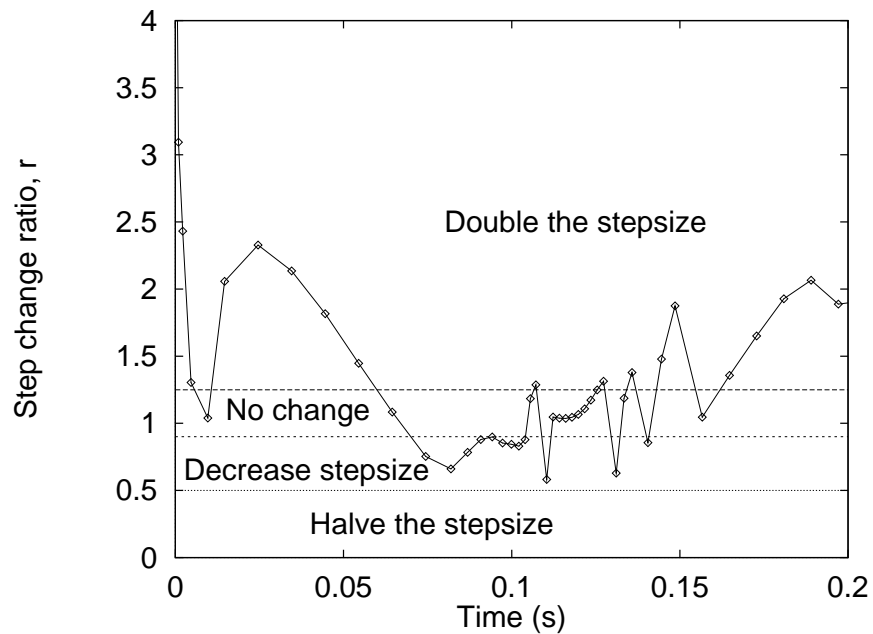
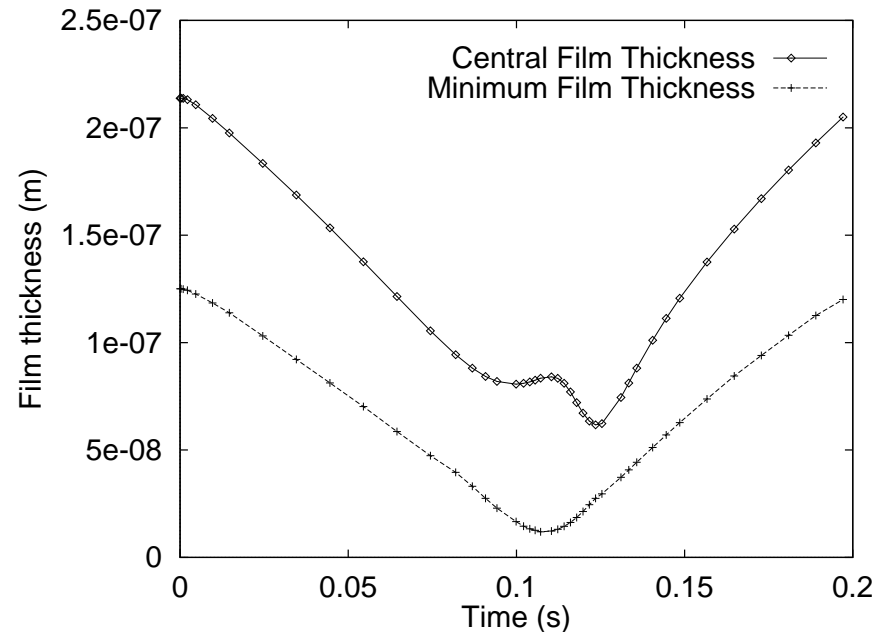


Plot of central and minimum film thickness

Transient EHL Problem - Reversal

Reversal from 0.05ms^{-1} to -0.05ms^{-1} in 0.2s.

Variable Time Stepping in Action



Parallelism - Why is it necessary for EHL?

- Industry is now after solutions to real surface roughness problems
- This will require meshes of 10000×10000 points
- Such large arrays cannot be stored – and worked with – on a single processor
- Parallelism will enable the work to be shared without compromising the accuracy
- Speed-ups for the current problems are easily attainable

Parallelism - How we do it using MPI

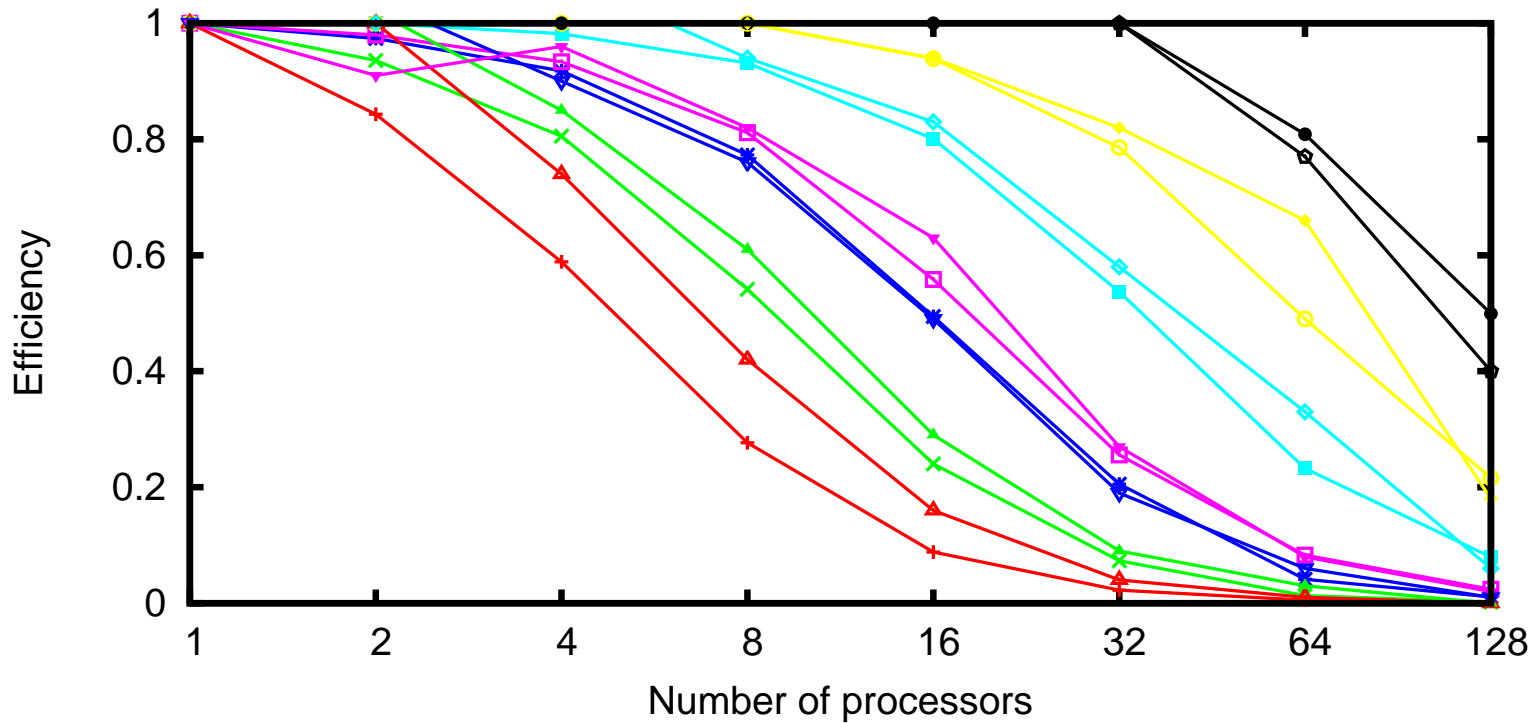
- The domain is divided into lengthwise strips for pressure, density and viscosity
 - This enables simple load balancing
 - The Reynolds Equation line based solution method is unchanged
 - Density and viscosity are local calculations and are only used for pressure
 - Communication is accomplished without extra effort
- The deformation calculation is done similarly - MLMI complicates matters
 - Ghost cells add an extra difficulty in getting both perfect load balancing and minimising communication
 - The coarsening requires global broadcasts
 - Strip division is fixed for the summation prolongation process to fix local communication costs (Top and bottom processors may be briefly idle)

Using Threads (in SCIRun) all communications are reduced to a single barrier.

Parallelism - MPI Timings (4097×4097)

Number of n_p	Snowdon		NGS		Memory		K_{sum}
	Time	Effic.	Time	Effic.	Mb	Iso-memory	Grid Used
1	-		-		2807		65x65
2	1520.87	1.00	1073.58	1.00	1413	0.99	65x65
4	701.71	1.08	554.05	0.97	713	0.98	65x65
8	402.81	0.94	278.07	0.97	363	0.97	65x65
16	228.59	0.83	146.91	0.91	188	0.93	65x65
32	163.25	0.58	98.67	0.68	101	0.87	65x65
64	142.93	0.33	79.96	0.42	59	0.74	128x128
128	410.41	0.06	237.40	0.07	41	0.53	256x256

Parallelism - Modelling the performance



		Points per grid				
Model	257x257			Actual	257x257	
Model	513x513			Actual	513x513	
Model	1025x1025			Actual	1025x1025	
Model	2049x2049			Actual	2049x2049	
Model	4097x4097			Actual	4097x4097	
Model	8193x8193			Actual	8193x8193	
Model	16385x16385			Actual	16385x16385	

Problem Solving Environments (PSEs)

PSEs are advantageous because they

- allow synchronous computation and visualisation
- can connect powerful visualisation tools to every dataset
- remove the need for much recompilation of codes
- allow users to change the problem being solved mid-stream

Dataflow often through a pipeline structure joining together modules for different tasks.

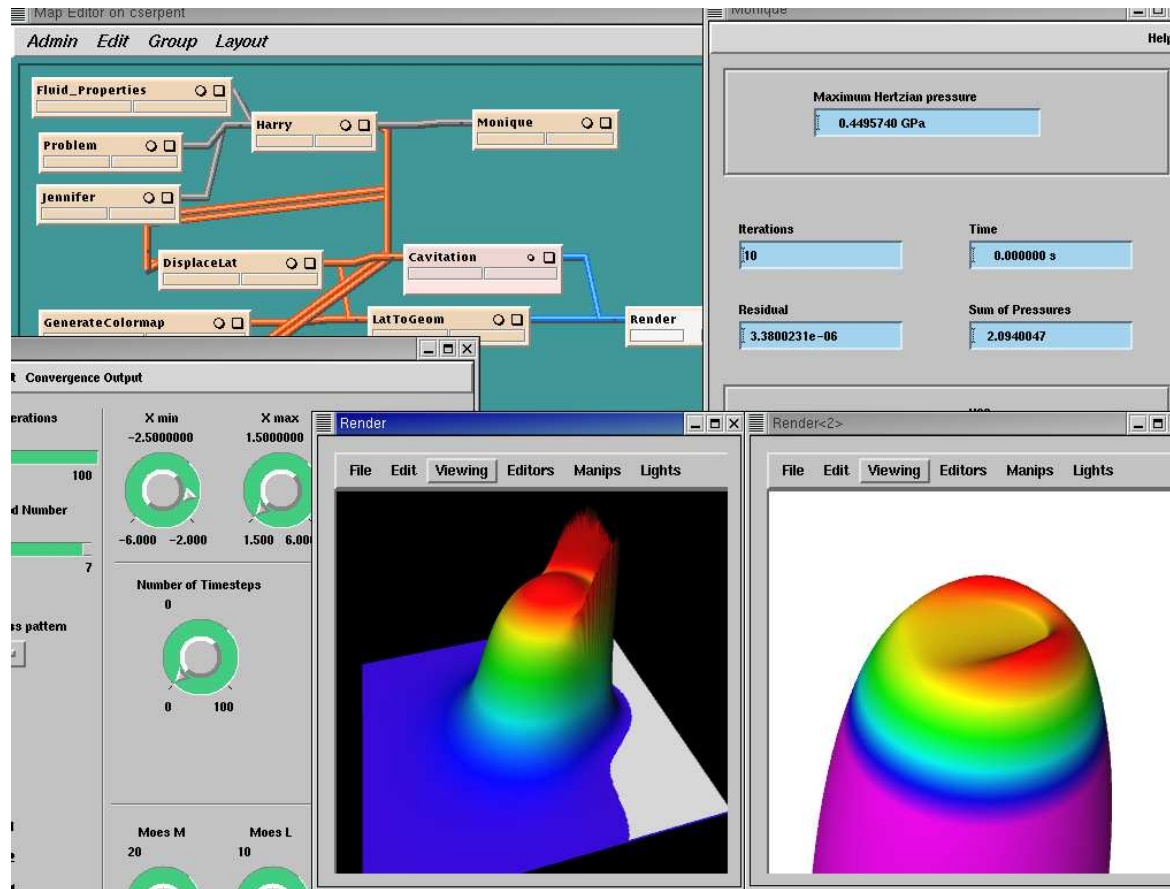
PSEs - Module Control Panel

The image shows a software control panel for PSEs (Particle Size Estimation) with various parameters and controls. The panel is divided into several sections:

- Level of Output / Convergence Output:** This section contains several control elements:
 - Max Iterations:** A slider set to 10, with a range from 1 to 100. An arrow labeled "Iterations" points to this slider.
 - Max Grid Number:** A slider set to 7, with a range from 3 to 7. An arrow labeled "Grid level" points to this slider.
 - Roughness pattern:** A dropdown menu currently set to "Ridge". An arrow labeled "Surface features" points to this menu.
 - X-offset:** A slider set to 0.0000000, with a range from -2.500 to 1.500.
 - Relaxation parameters:** Three radio buttons with values 0.1, 0.2 (selected), and 0.4. An arrow labeled "Relaxation parameters" points to the 0.2 option.
 - Run:** A button to execute the simulation.
 - Loop:** A dropdown menu currently set to "Initialise". An arrow labeled "Steering capabilities" points to this menu.
- Domain size:** Three circular gauges representing the domain boundaries:
 - X min:** -2.5000000
 - X max:** 1.5000000
 - Ymax:** 2.0000000An arrow labeled "Domain size" points to these gauges.
- Transient options:** Two circular gauges representing transient simulation parameters:
 - Number of Timesteps:** 6
 - Timestep Size:** 0.0010000000An arrow labeled "Transient options" points to these gauges.
- Transient case:** A dropdown menu currently set to "Surface features".
- Non-dimensional parameters:** Three circular gauges representing non-dimensional parameters:
 - Moes M:** 35
 - Moes L:** 10
 - Material G:** 4700.0000An arrow labeled "Non-dimensional parameters" points to these gauges.

PSEs - ECLIPSE in IRIS Explorer

IRIS Explorer is a commercial “visual programming environment for customised visualisation applications” – NAG.



The Grid and IRIS Explorer

- IRIS Explorer modules can be used to launch other processes:
 - on the same machine as the visualisation
 - somewhere else on the network
 - on the Grid (using Globus)

All of these may be parallel jobs

- Communication is done through the gViz library:
 - Input parameters can be taken from the widgets
 - Input data can come from other input modules
 - Output data is released for visualisation
- As a separate job is started (and left running) then the local machine can focus on the visualisation

Shell's Optimisation Application

- Wish to find set of lubricant model parameters (e.g. viscosity, pressure, temperature coefficients) which best match observed data
- Typically over 10 such parameters to optimise
- Physical observations already taken for different loadings (3), ambient temperatures (2) and slide:roll ratios (6)

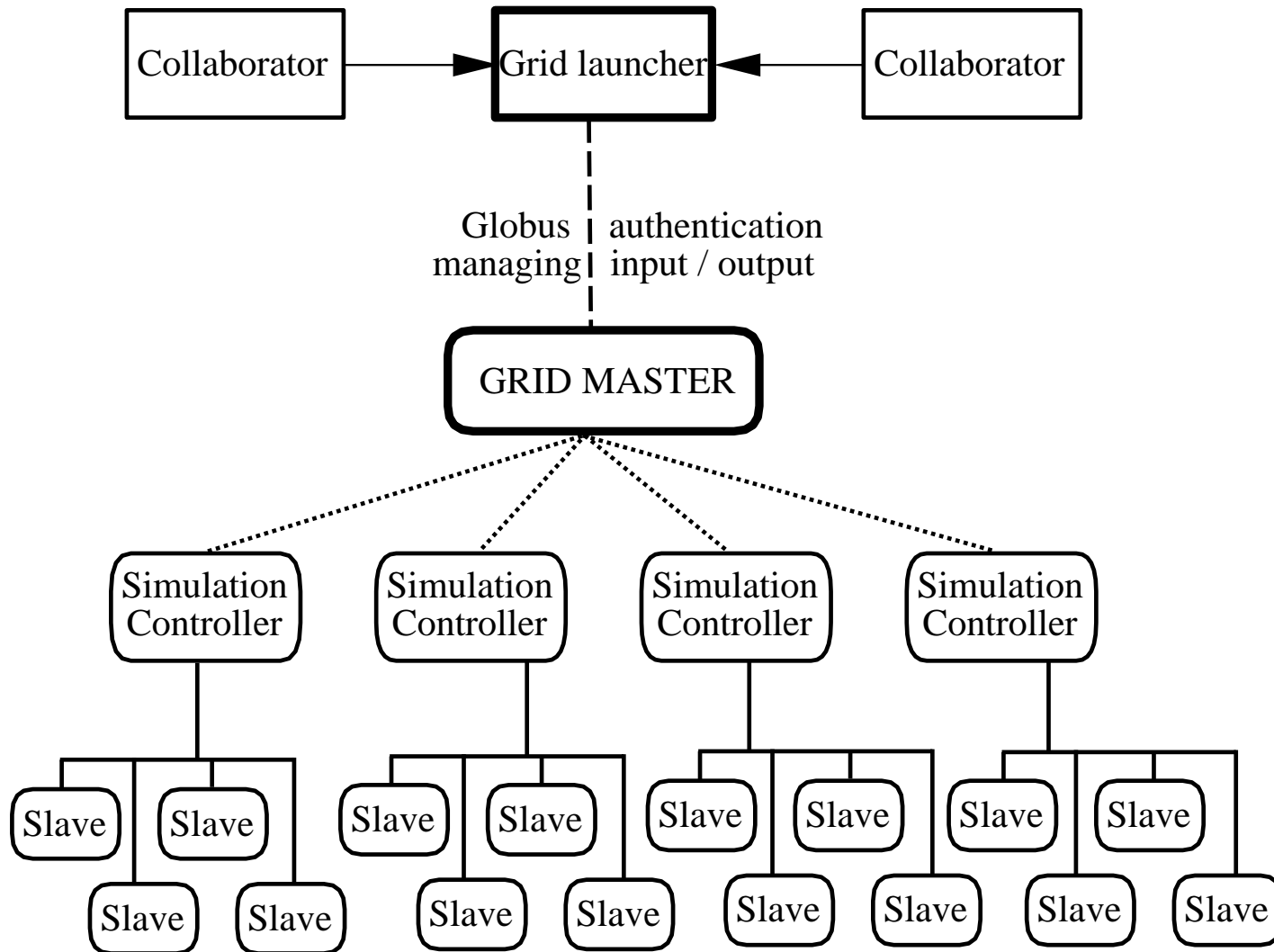
Therefore must perform non-linear optimisation of

$$\mathcal{R}_F = \sum_{j=1}^{36} \left(F_j^{num} - F_j^{exp} \right)^2$$

⇒ Each \mathcal{R}_F evaluation needs 36 numerically expensive EHL calculations.

- Shell uses a simplex method to optimise

Hierarchical Parallelism on the Grid



Summary I

- Line and Point contact EHL solutions have been solved for the following cases
 - Steady: Newtonian, generalised Newtonian, non-Newtonian, thermal
 - Transient: Newtonian, generalised Newtonian, thermal cases with
 - * Surface roughness
 - * Variable loads
 - * Variable rolling speeds
 - * Variable contact radii
- Fast multilevel schemes have been used on meshes up to $\frac{1}{4}$ billion points
- Adaptive meshes have been used
- Discontinuous Galerkin finite elements
- Adjoint calculations for quantities of interest
- Variable timestepping has been introduced

Summary II

- Problem Solving Environments for EHL have been constructed
 - Both IRIS Explorer and SCIRun have been successfully used
- Parallelism has been used for multilevel calculations
 - Both MPI and thread based versions were devised
- The PSE has been Grid enabled from within IRIS Explorer
 - Input data can be taken from the control panel for from input modules
 - Output data is visualised outside of Grid resources
 - Steering capabilities still present
- Hierarchical parallelism of an optimisation code, with the EHL solver as the work unit, has been implemented

Future Work

- Transient rheological models
- Realistic surface roughness

Future Work

- Transient rheological models
- Realistic surface roughness